ACS POLYMERS Au
AN OPEN ACCESS JOURNAL OF THE AMERICAN CHEMICAL SOCIETY

pubs.acs.org/polymerau
Article

Highly Stretchable Stress–Strain Sensor from Elastomer Nanocomposites with Movable Cross-links and Ketjenblack

Ryohei Ikura, Kota Kajimoto, Junsu Park, Shunsuke Murayama, Yusei Fujiwara, Motofumi Osaki, Tomohiro Suzuki, Hidenori Shirakawa, Yujiro Kitamura, Hiroaki Takahashi, Yasumasa Ohashi, Seiji Obata, Akira Harada, Yuka Ikemoto, Yuta Nishina,* Yasutomo Uetsuji,* Go Matsuba,* and Yoshinori Takashima*

Cite This: ACS Polym. Au 2023, 3, 394–405

Read Online

ACCESS | Metrics & More | Article Recommendations | Supporting Information

ABSTRACT: Practical applications like very thin stress–strain sensors require high strength, stretchability, and conductivity, simultaneously. One of the approaches is improving the toughness of the stress–strain sensing materials. Polymeric materials with movable cross-links in which the polymer chain penetrates the cavity of cyclodextrin (CD) demonstrate enhanced strength and stretchability, simultaneously. We designed two approaches that utilize elastomer nanocomposites with movable cross-links and carbon filler (ketjenblack, KB). One approach is mixing SC (a single movable cross-network material), a linear polymer (poly(ethyl acrylate), PEA), and KB to obtain their composite. The electrical resistance increases proportionally with tensile strain, leading to the application of this composite as a stress–strain sensor. The responses of this material are stable for over 100 loading and unloading cycles. The other approach is a composite made with KB and a movable cross-network elastomer for knitting dissimilar polymers (KP), where movable cross-links connect the CD-modified polystyrene (PSCD) and PEA. The obtained composite acts as a highly sensitive stress–strain sensor that exhibits an exponential increase in resistance with increasing tensile strain due to the polymer dethreading from the CD rings. The designed preparations of highly repeatable or highly responsive stress–strain sensors with good mechanical properties can help broaden their application in electrical devices.

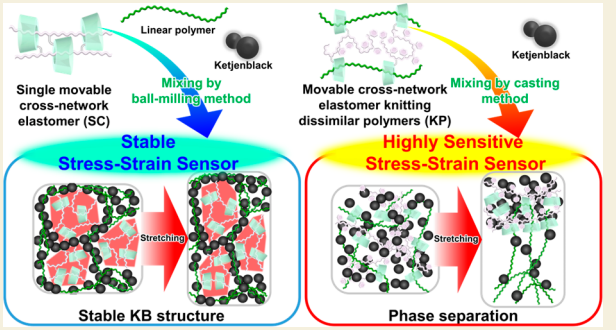

KEYWORDS: *stress–strain sensor, carbon composite, movable cross-link, supramolecular materials, polymeric materials, tough materials, upcycling*

Flexible stress–strain sensors have attracted considerable attention due to increasing demands for their application in wearable electronic devices,[1−3] for structural health monitoring[4,5] and human motion detection,[6] and in soft robotics.[7,8] The main strain sensing outputs are mechanochromism[5,9−18] and electrical signals. The methods to transduce mechanical deformation into electrical signals include resistive change,[19] piezoelectricity,[20−24] triboelectricity,[6,25] capacitive response,[26−29] transistor,[24,30,31] and macroscopic shape change.[32−36] Traditional metallic and semiconducting stress–strain sensors show excellent sensitivity but low flexibility due to low fracture strain (<5%).[37,38] Compositing polymeric and conductive materials (e.g., carbon black,[39−44] carbon nanotubes,[45−54] graphene,[55−62] metal nanofillers,[63−71] liquid metals,[8,72] conductive polymers,[73−75] MXenes,[76] and ionic liquids[77−79]) is an effective method to achieve high stretchability. The types of stress–strain sensors that utilize the above composites mainly employ the resistive change caused by the disconnection of conductive paths. Practical applications like very thin stress–strain sensors require high strength, stretchability, and conductivity, simultaneously. To achieve them, one of the important approaches is improving the toughness of stress–strain sensing materials. However, it is usually difficult to improve the strength and stretchability of the general polymeric materials simultaneously.

Recently, a lot of effort has been put into overcoming issues mentioned above. Polymeric materials with high strength and stretchability have been designed via three approaches. One approach is the use of interpenetrating brittle and ductile networks.[14,80−83] Another approach is the use of a reversible cross-linked network. Notably, these approaches are based on

Received: April 29, 2023
Revised: August 30, 2023
Accepted: August 31, 2023
Published: September 11, 2023

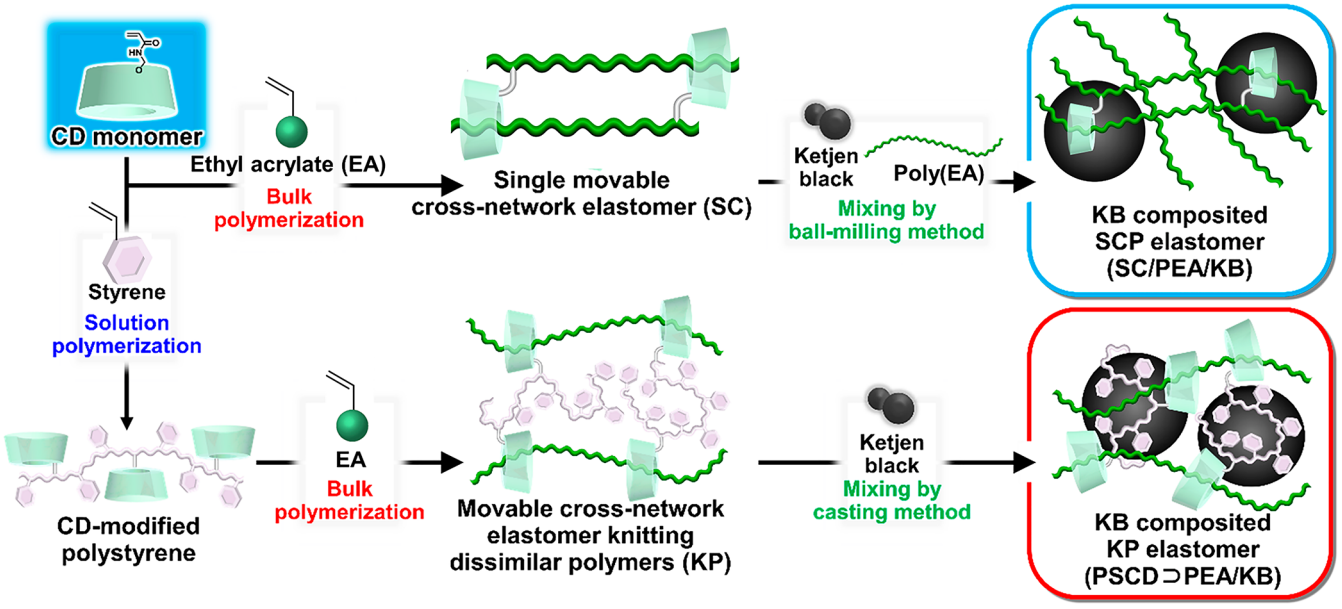

Figure 1. Routes for two different material designs: KB-composited SCP elastomer (SC/PEA/KB) and KB-composited KP elastomer (PSCD⊃PEA/KB).

sacrificial bonds, which dissipate stress to prevent catastrophic crack propagation.[84−96] The final approach is the use of a movable cross-linked network that disperses stress based on the mobility of cross-links along the axis of the polymers.[97−110] This stress dispersion strategy results in high toughness.

Previously, we prepared elastomers with movable cross-links as stress dispersion units by the copolymerization of cyclodextrin (CD) and vinyl monomers.[108,109] The vinyl chain polymers penetrated into the CD cavities to form movable cross-links, and the obtained elastomers showed a higher fracture stress and strain than those of covalently cross-linked elastomers.

We hypothesize that compositing these movable cross-linked elastomers and conductive materials by suitable methods will realize innovative stress−strain sensors with high strength, stretchability, electrical conductivity, and sensitivity. The stress−strain sensors constructed by a combination of hard and soft domains are expected to have excellent mechanical and electrical properties. On the basis of our hypothesis, we focus on the mechanical and electrical properties of composite materials with a carbon filler (ketjenblack, KB) and two types of movable cross-linked elastomers to realize high repeatability or sensitivity of strain sensing (Figure 1). One composite consists of SCP (single movable cross-network (SC) elastomer with a penetrating polymer) elastomers with KB and is obtained by ball-milling methods. The SCP composites consist of soft SC elastomer particles and hard networks of linear polymers with KB, abbreviated SC/PEA/KB. The other composite consists of movable cross-network elastomers for knitting dissimilar polymers (KP) with KB (PSCD⊃PEA/KB), where PEA polymers penetrate the CD-modified polystyrene, acting as the movable cross-links. The movable cross-links connect the hard and soft polymers to achieve high strength and stretchability.

EXPERIMENT AND METHODS

Preparative details of the polymers and KB composites can be found in the Supporting Information. Methodological details of characterization of the polymers and KB composites by nuclear magnetic resonance (NMR), Fourier transform infrared (FT-IR), and Raman spectra, gel permeation chromatography (GPC), mechanical properties measurements, and electrical conductivity measurements (ultrasmall angle X-ray scattering (USAXS) measurement, small-angle X-ray scattering (SAXS) measurement, scanning electron microscopy (SEM)) can be found in the Supporting Information.

RESULTS AND DISCUSSIONS

Preparation of the KB Composites (SC/PEA/KB(*w*) and PSCD⊃PEA/KB(*w*))

Figures 2a, 3a, and S3 show the chemical structures of the vinyl monomers, primary polymers, KP elastomers, SC elastomers, and polymer blends. Ethyl acrylate (EA), styrene (S), and *N*,*N*-dimethylacrylamide (DMAA) were employed as liquid vinyl monomers. The peracetylated γCD monomer (mono-6*O*-acrylamidomethyl-triicosaacetyl-γ-cyclodextrin, TAcγC-DAAmMe) was solubilized in hydrophobic solvents. Ketjenblack (KB) was composited as a carbon filler.

Schemes S1 and S6 show the preparation of SC elastomers and linear polymer PEA. SC elastomers with permanent cross-links are not dissolved into solvents but are swollen to form organogels. SC/PEA/KB(*w*) (*w* is the wt % of KB) was obtained by mixing SC, linear polymer PEA, and KB with *N*-methyl pyrrolidone (NMP) using a ball-milling method (Schemes S7, S9, and S10; Tables S3 and S9). This method kinetically mixes the samples and zirconia balls through the use of severe shear stress during planetary movement. These balls crush the SC organogels, resulting in well-mixed slurries. After the NMP is removed, the obtained KB composites are abbreviated SC/PEA/KB(*w*). As control samples to investigate the properties derived from network structures, SC/PEA without KB, PEA/KB(*w*), and SC/KB(*w*) were also prepared by the ball-milling methods.

Schemes S2−S5 and Tables S1−S2 show the preparation of PSCD⊃PEA (KP elastomers) and PS/PEA (polymer blends as control samples). PSCD⊃PEA elastomers were dissolved into tetrahydrofuran (THF) to dethread the after-polymerized PEA chain (secondary polymer). Casting a THF suspension of KP elastomers and KB resulted in PSCD⊃PEA/KB(*w*), where *w* is

https://doi.org/10.1021/acspolymersau.3c00010
ACS Polym. Au 2023, 3, 394−405

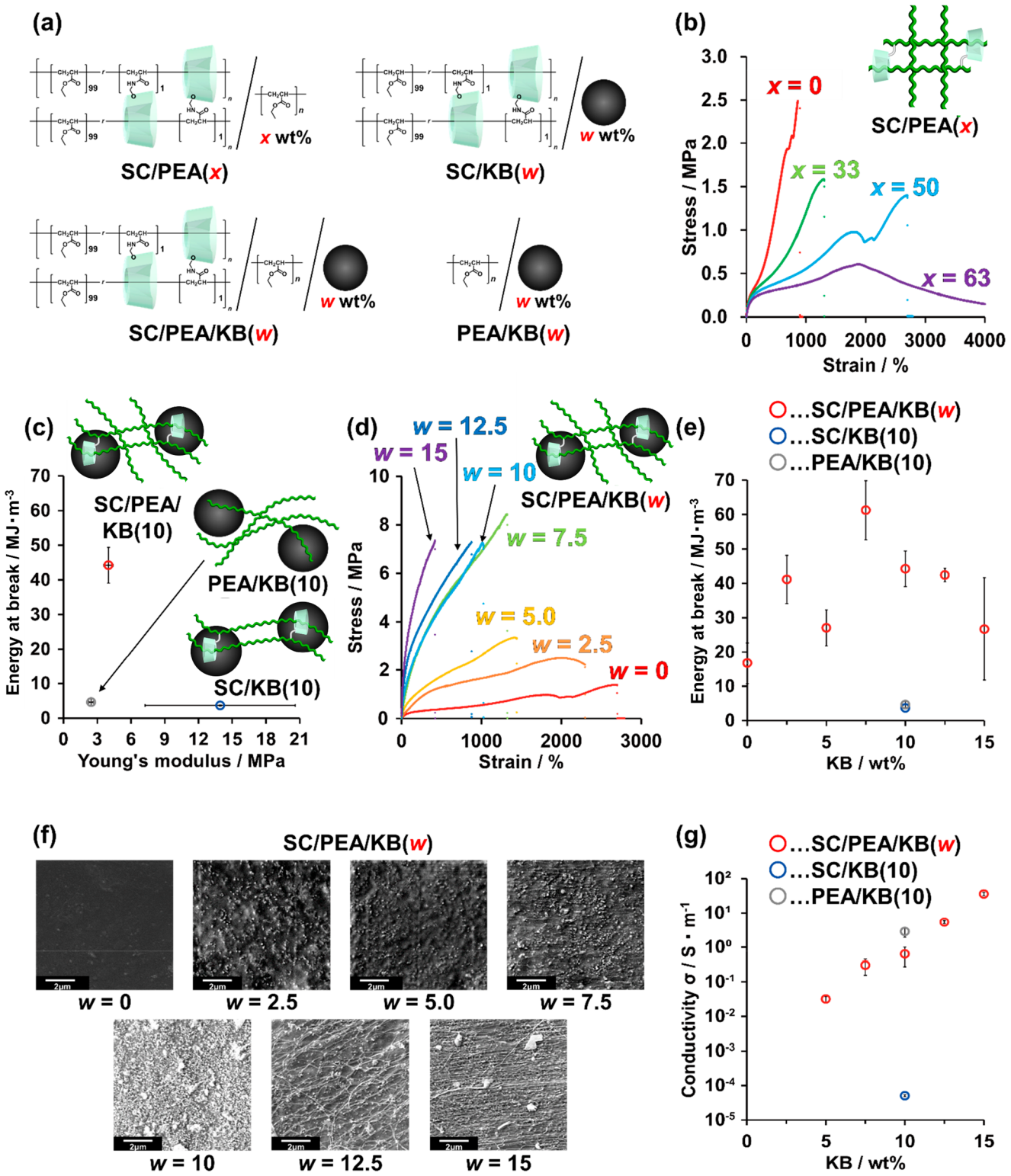

Figure 2. (a) Chemical structures of SC/PEA(x), SC/PEA/KB(w), SC/KB(w), and PEA/KB(w). (b) Stress−strain curves of SC/PEA(x) (x = 0, 33, 50, and 63). (c) Plots of the energy at break and Young's modulus values of SC/PEA/KB(10), PEA/KB(10), and SC/KB(10). (d) Stress−strain curves and (e) plots of the energy at break and wt % values of KB. (f) Cross-section SEM images of SC/PEA/KB(w) (w = 0, 2.5, 5.0, 7.5, 10, 12.5, and 15 wt %) at 1,000× magnification. (g) Plots of the conductivity and wt % of the KB in SC/PEA/KB(w) (w = 0, 2.5, 5.0, 7.5, 10, 12.5, and 15 wt %), PEA/KB(10), and SC/KB(10).

wt % of KB (Scheme S8; Tables S4−S6). PSCD⊃PEA without KB and PS/PEA/KB(w) were also prepared in the same manner. The obtained materials were characterized by ^{1}H NMR, ^{13}C NMR, FT-IR, and Raman spectra (Figures S4−S33).

https://doi.org/10.1021/acspolymersau.3c00010
ACS Polym. Au 2023, 3, 394−405

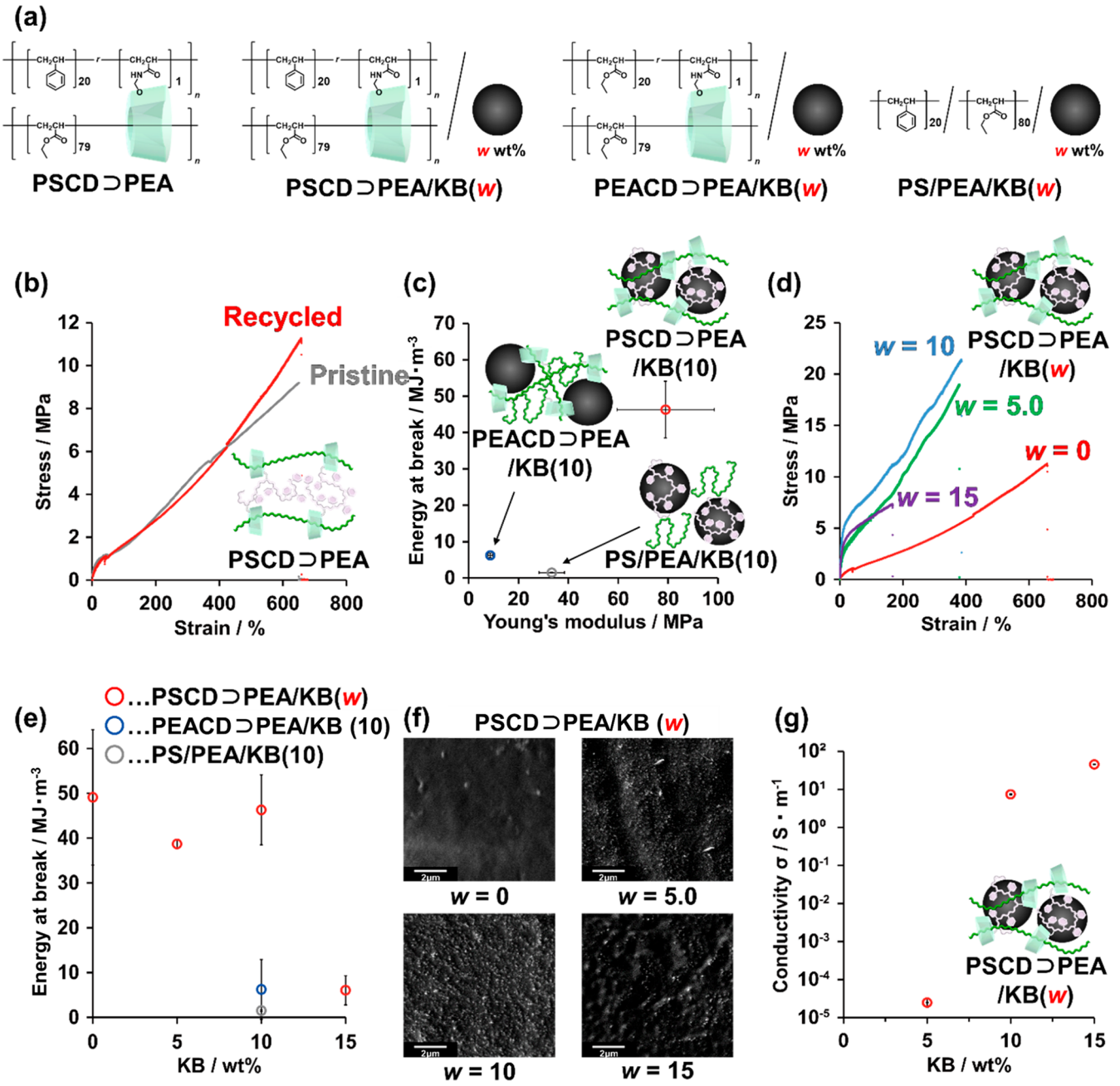

Figure 3. (a) Chemical structures of PSCD⊃PEA, PSCD⊃PEA/KB(w), PSCD/PEA/KB(w), and PEACD⊃PEA/KB(w). (b) Stress−strain curves of pristine and recycled PSCD⊃PEA. (c) Plots of the energy at break and Young's modulus of PSCD⊃PEA/KB(10), PSCD/PEA/KB(10), and PEACD⊃PEA/KB(10). (d) Stress−strain curves of PSCD⊃PEA/KB(w) (w = 0, 5.0, 10, and 15 wt %). (e) Plots of the energy at break and wt % of KB. (f) SEM images at 10,000× magnification. (g) Plots of the conductivity and wt % of PSCD⊃PEA/KB(w) (w = 0, 5.0, 10, and 15 wt %).

Mechanical Properties of SC/PEA

Prior to KB compositing, the mechanical properties of SC/PEA(x) elastomers were optimized by investigating polymer network structures with various wt % of PEA (x = 0, 33, 50, and 63 wt %). The mechanical properties of the SC/PEA(x) elastomers were evaluated by tensile tests (Figures 2b and S35), and energy at break was calculated from the integral of the stress−strain curve. As a result, the fracture strain increased with increasing x values. SC/PEA(33) and SC/PEA(50) showed clear fracture points, suggesting a network structure with physical cross-links based on entanglements with linear polymers penetrating the SC networks. The stress of SC/PEA(63) started decreasing over approximately 2,000% strain, indicating that the necking by the disentanglements of linear polymers dispersed the stress at high strain. SC/PEA(50) also showed the necking around 2,000% strain. Notably, SC/PEA(50) had a good balance between elasticity and stress dispersion to achieve the highest energy at break (17 ± 6 MJ·m^{-3}). The cyclic tensile test of SC/PEA(50) shows the elasticity in low strain and stress-dispersion in high strain, allowing for improving the fracture strain and stress simultaneously (Figure S36). Hereinafter, the KB composite materials for stress−strain sensors were optimally prepared with 50 wt % linear polymers.

https://doi.org/10.1021/acspolymersau.3c00010
ACS Polym. Au 2023, 3, 394−405

Mechanical Properties of SC/PEA/KB(*w*)

Figure 2c shows plots of the relation between the energy at break and Young's modulus of SC/PEA/KB(10) and the control samples. PEA/KB(10) showed plastic deformation and low fracture stress due to the absence of cross-links (Figure S37 and S38). SC/KB(10) was not well mixed between the SC network and KB, leading to the lowest energy at break. On the other hand, SC/PEA/KB(10) exhibited clear fracture points and the highest energy at break (44 ± 5 MJ·m^{-3}). These results indicated the presence of a network structure in SC/PEA/KB(10), resulting from entanglements between the SC networks and linear polymer. These structures contributed to improving the mechanical properties and mixabilities. This presumption was also supported by the plastic deformation and low energy at break of SC/PS/KB(10), where entanglements between the immiscible main chains (PEA and PS) could not form due to their low miscibility (<0.01 wt % of PEA in PS)[111] (Figure S39).

Figure 2d shows the stress−strain curves of the SC/PEA/KB(*w*) composites with various KB content (*w* = 0, 2.5, 5.0, 7.5, 10, 12.5, and 15 wt %). The results can be divided into two tendencies. (i) At low wt % of KB (*w* = 0, 2.5, and 5.0), an increase in *w* resulted in higher fracture stresses and lower fracture strains. (ii) The other composites (*w* = 7.5, 10, 12.5, and 15 wt %) showed similar fracture stresses, whereas their fracture strains decreased with increasing *w*. The fracture stress of SC/PEA/KB(7.5) significantly increased to 2.4 ± 0.3 times that of SC/PEA/KB(5), yielding the highest energy at break (61 ± 9 MJ·m^{-3}) (Figure 2e). These results suggested structural changes of KB aggregates around *w* = 7.5 wt %.

Scanning electron microscopy (SEM) was used to observe the morphology of KB in the composites (Figure 2f). As a result, fibril-like structures were observed from the composites with a high wt % of KB (*w* = 7.5, 10, 12.5, and 15 wt %). Considering the fibrillar structures increase with wt % of KB, the fibrillar structures seem to be the KB-rich domains with PEA. During the ball-milling, the KB-rich domains may be stretched to form the fibrillar structures. These results confirmed the structural change around *w* = 7.5 wt %, leading to a high fracture stress. In addition, long fibril-like structures (>3 μm) were observed from SC/PEA/KB(12.5) and SC/PEA/KB(15). This would contribute to the drastic increase in their Young's moduli (Figure S38).[112]

Electrical Properties of SC/PEA/KB(*w*)

Figure 2g shows the relation between the electrical conductivity and *w* of SC/PEA/KB(*w*), SC/KB(10), and PEA/KB(10) by the four-point probe method. The conductivity of SC/PEA/KB(2.5) was too low to be measured ($\sigma < 10^{-5}$ S·m^{-1}), while the conductivity of SC/PEA/KB(5) suddenly increased to 0.05 S·m^{-1}. Furthermore, the conductivities of SC/PEA/KB(*w*) (*w* = 5.0, 7.5, 10, 12.5, and 15 wt %) exponentially increased with *w*, indicating that the formation of conductive paths started at 2.5 < *w* < 5. The SEM images showed that the increase in *w* resulted in the growth of fibril-like structures rather than sea−island structures, allowing the exponential increase in conductivity. SC/PEA/KB(10) exhibited a 1.7 × 10^4-fold increase in the conductivity of SC/KB(10). Considering the conductivity of PEA/KB(10) is higher than that of SC/PEA/KB(10), the linear polymer in SC/PEA/KB(10) resulted in good mixing and high conductivity. USAXS profiles show the similar size of KB aggregations (30−300 nm) in SC/PEA/KB(10) and PEA/KB(10), indicating that PEA domains in SC/PEA/KB(10) give good mixability to achieve a high conductivity (Figure S43a). Consequently, the network structure with linear polymers penetrating the SC networks leads to materials for stress−strain sensors with high toughness and conductivity.

Recyclability of PSCD⊃PEA

PSCD⊃PEA/KB(*w*) composites were prepared by a casting method. When KP elastomers are dissolved in solvents, movable cross-links dissociate via the dethreading of secondary polymers from the TAcγCD unit. Notably, the GPC profiles of the PSCD⊃PEA solutions showed two peaks with a molecular weight order comparable to that of the (i) PS-CD primary polymers and (ii) PEA obtained by bulk polymerization (Figure S34; Tables S7 and S8). Therefore, it is necessary to ensure the reformation of movable cross-links through the removal of THF in casting methods.

Figure 3b shows the stress−strain curves of the pristine PSCD⊃PEA elastomers and recycled elastomers obtained by casting methods using THF. The pristine and recycled samples showed similar stress−strain curves, indicating the high recyclability of PSCD⊃PEA. The recycled PSCD⊃PEA showed a Young's modulus of 87 ± 10% of that of pristine PSCD⊃PEA, showing the effective restoration of the cross-links. The ^{1}H−^{1}H Nuclear Overhauser effect spectroscopy (NOESY) NMR results of the recycled films revealed the reformation of movable cross-links (Figure S44). These results demonstrate the recyclability of PSCD⊃PEA based on the reformation of movable cross-links via the rethreading of secondary polymers. The recyclability enables the acquisition of KB composite materials by casting methods without impairing their cross-links and Young's moduli.

Mechanical and Electrical Properties of PSCD⊃PEA/KB(*w*)

Figure 3c shows plots of the relation between the energy at break and Young's modulus of PSCD⊃PEA/KB(10) and the control samples. The composite without cross-linked PS/PEA/KB(10) showed plastic deformation, low energy at break, and a rough surface due to phase separation based on the low miscibility of the PS and PEA main chains (Figure S38). The phase separation brings the heterogeneous distribution of KB, resulting in the rough surface. In contrast, PSCD⊃PEA/KB(10) showed clear fracture points, a smooth surface, a 30 ± 5-fold increase in energy at break, and a 2.4 ± 0.6-fold increase in the Young's modulus of PS/PEA/KB(10), showing that the reformation of movable cross-links improved the mechanical properties and mixability.

Interestingly, PSCD⊃PEA/KB(10) exhibited a 7.4 ± 1.3-fold increase in energy at break and a 9.1 ± 2.2-fold increase in the fracture strain of PEACD⊃PEA/KB(10) with PEA as the primary polymer. Contrary to PSCD⊃PEA/KB(10), PEACD⊃PEA/KB(10) showed a rough surface. These results indicated that PS polymers contributed to the improvement in the mechanical properties and mixability. The USAXS profile of PEACD⊃PEA/KB(10) showed high intensity, indicating high heterogeneity due to poor mixability. However, USAXS profiles of PSCD⊃PEA/KB(10) and PS/PEA/KB(10) exhibit the peak of dispersed KB monoparticles (30 nm), supporting that PS polymers give good mixability (Figure S43b).

Figure 3d shows the stress−strain curves of the PSCD⊃PEA/KB(*w*) composites with various wt % of KB (*w* = 0, 5.0, 10, and 15 wt %). PSCD⊃PEA/KB(5) and PSCD⊃PEA/KB(10) showed higher fracture stress and lower fracture strain than PSCD⊃PEA without KB. From *w*

https://doi.org/10.1021/acspolymersau.3c00010
ACS Polym. Au 2023, 3, 394−405

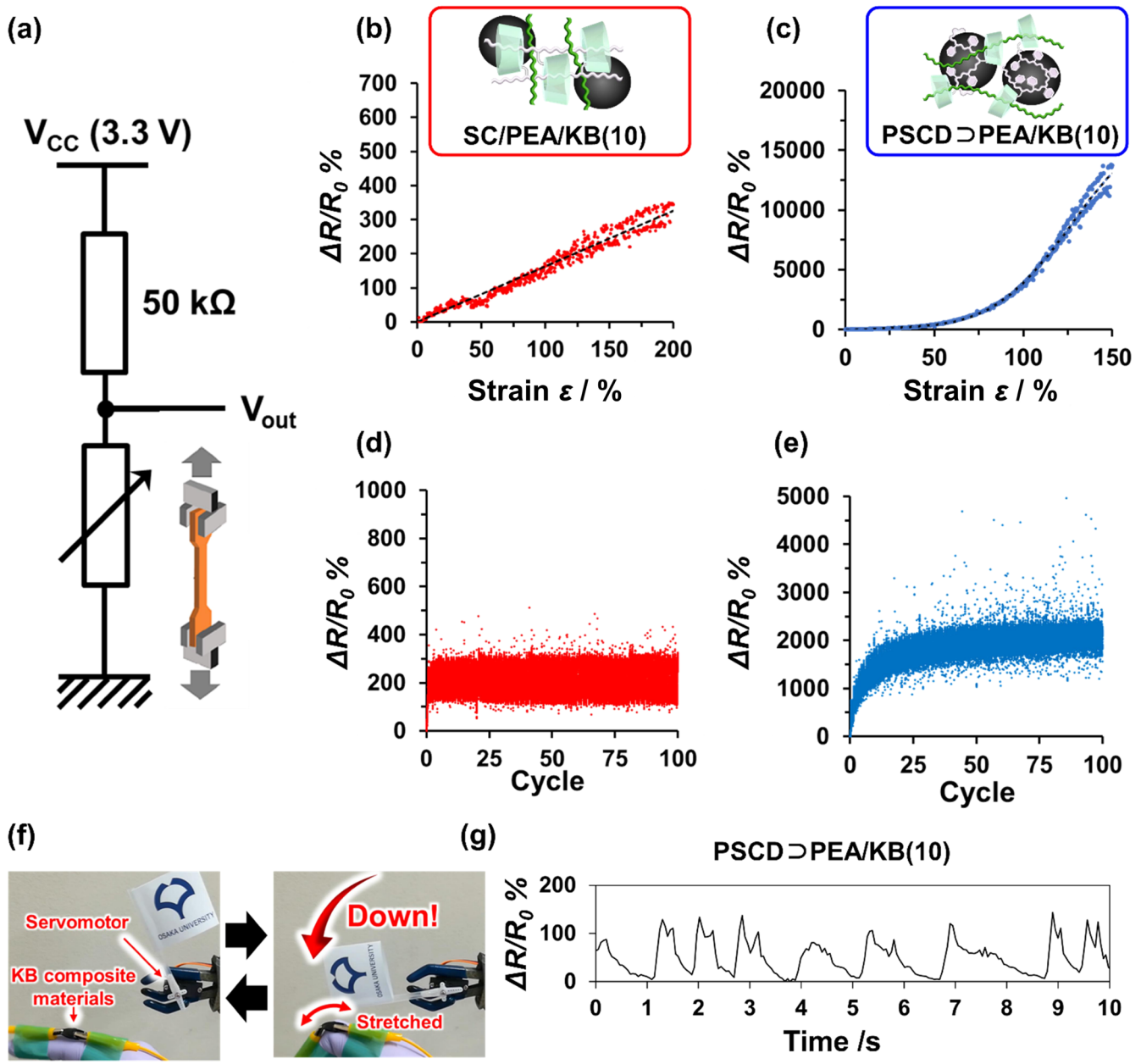

Figure 4. (a) Circuit for real-time electrical conductivity measurements of the KB composites upon tensile deformation. $\Delta R/R_0$ values of (b) SC/PEA/KB(10) and (c) PSCD⊃PEA/KB(10) upon tensile deformation. $\Delta R/R_0$ of (d) SC/PEA/KB(10) and (e) PSCD⊃PEA/KB(10) during 100 stretch-release cycles at 100% strain. (f) Photographs of the stress−strain sensing and remote actuating system are from Movie S1. This system was designed so that the servomotor operated in response to changes in the resistance of PSCD⊃PEA/KB(10) attached to a finger. (g) Changes in the resistance of PSCD⊃PEA/KB(10) by finger movements. The blue ginkgo logo in Figure 4f is the symbol of Osaka University. The logo is a copyright and has been licensed for use by Osaka University.

= 0−10 wt %, an increase in w resulted in a similar energy at break but higher Young's modulus (Figures 3e and S39). Notably, PSCD⊃PEA/KB(15) showed a rough surface with the smallest fracture stress and strain. In addition, the Young's modulus of PSCD⊃PEA/KB(15) was smaller than that of PSCD⊃PEA/KB(10), indicating that the association between the matrix polymers and KB did not work well.

Figure 3g shows the relation between the electrical conductivity and w of PSCD⊃PEA/KB(w). From w = 0−10 wt %, the increase in w resulted in a drastic increase in electrical conductivity. However, PSCD⊃PEA/KB(15) exhibited a moderate increase. These results suggested structural changes between w = 10 and 15 wt %. In the SEM images of PSCD⊃PEA/KB(5) and PSCD⊃PEA/KB(10), many dispersed KB domains were observed on the surface (Figure 3f). These dispersed KB domains improved the fracture stress and Young's modulus without lowering the energy at break. However, PSCD⊃PEA/KB(15) showed aggregated structures, resulting in poor mechanical properties. Consequently, PSCD⊃PEA/KB(10) is a good candidate for stress−strain sensors with high energy at break, Young's modulus, and conductivity.

https://doi.org/10.1021/acspolymersau.3c00010
ACS Polym. Au 2023, 3, 394−405

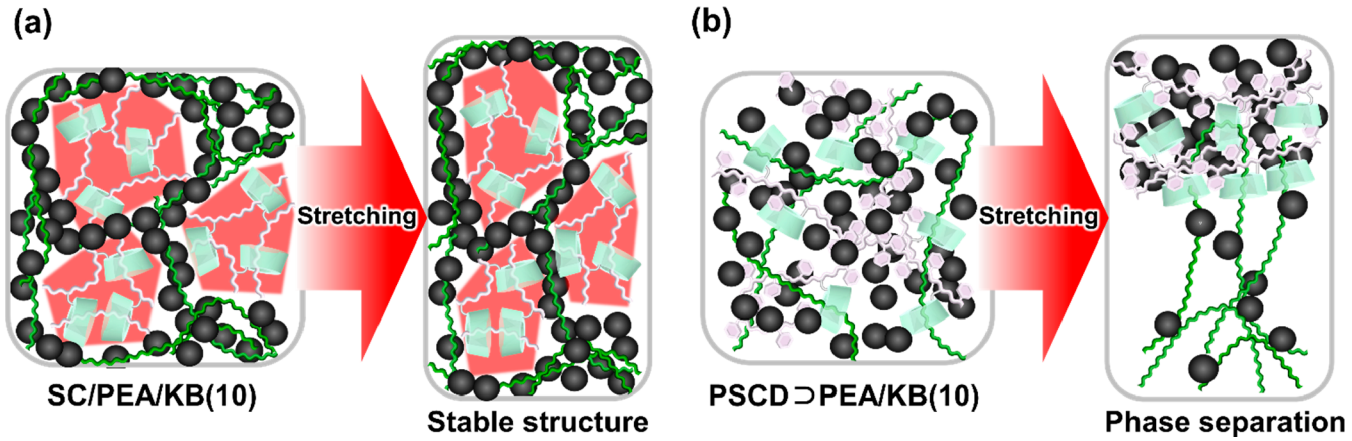

Figure 5. Proposed structures of (a) SC/PEA/KB(10) and (b) PSCD⊃PEA/KB(10).

Electrical Properties upon Deformation and Application for Stress–Strain Sensors

To investigate the potential for the application of stress–strain sensors, real-time measurements of the electrical conductivity of each KB composite upon tensile deformation were performed using the circuit shown in Figure 4a and S45. The resistances of the KB composite (R) were measured and calculated with Equation 1, where V_{out} is the voltage at junction between the 50 kΩ resistor and the KB composites. All the voltage was measured using ground in the circuit as reference (0 V).

$$R = \frac{50\ \text{k}\Omega \times V_{out}}{3.3\ \text{V} - V_{out}} \quad (1)$$

The relative changes in the resistance ($\Delta R/R_0$) were obtained with Equation 2, where R_0 is the initial resistance before deformation.

$$\Delta R/R_0 = \frac{R - R_0}{R_0} \times 100\% \quad (2)$$

Figure 4b shows the $\Delta R/R_0$ of SC/PEA/KB(10) upon stretching. The $\Delta R/R_0$ of SC/PEA/KB(10) proportionally increased with increasing strain. The gauge factor (GF) was 1.6 in the whole sensing range (Figure S46a). Figure 4d shows the $\Delta R/R_0$ of SC/PEA/KB(10) during 100 stretch-release cycles at 100% strain for a durability test. After several cycles, SC/PEA/KB(10) showed stable responses and repeatability as a stress–strain sensor. These results suggested that smaller structural changes occurred with tensile deformation. On the other hand, the $\Delta R/R_0$ of PSCD⊃PEA/KB(10) showed a large increase when stretched (Figure 4c). PSCD⊃PEA/KB(10) showed a 2.6-fold greater GF of SC/PEA/KB(10) at low strain ε = 0–20% (Figure S46b). Furthermore, GF increased with ε, reaching GF = 180 at ε = 100–120% (Figure S46c–e). After 100 stretch–release cycles, PSCD⊃PEA/KB(10) showed an increase in its $\Delta R/R_0$ and approached stable responses. These results suggested that the high sensitivity was caused by stress-induced structural changes (Figure 4e).

The high sensitivity of PSCD⊃PEA/KB(10) allows for its application as a stress–strain sensor and a remote actuator. The stress–strain sensing and remote actuating system was designed so that the servomotor operated in response to changes in the resistance of the KB composites attached to a finger (Figure 4f). When the finger was bent, the KB composite materials were stretched, causing an increase in resistance and lowering of the flag. When the finger was straightened, the strain was released, causing a decrease in the resistance and raising of the flag. Movie S1 demonstrates the successful control of flag movement according to finger movements and subsequent changes in resistance (Figure 4g). The three responses in 1–4 s indicate the small response time (Figure S46f), enabling the stress–strain sensing and remote actuating system.

Investigation of Strain-Sensing Mechanism by SAXS Measurements upon Tensile Deformation

To reveal the strain-sensing mechanism, SAXS measurements were performed upon tensile deformation. The profiles in the tensile and perpendicular directions were obtained from the scattering patterns at various strains (ε = 0%, 40%, 80%, 120%, 160%, and 200% strain). Whereas SC/PEA showed streaklike scattering in its SAXS profile, SC/PEA/KB(10) showed almost no change in its SAXS profile (Figure S47). These results indicated that the stable KB network structures suppressed the orientation of the polymer chain, resulting in stable and repeatable strain sensing of SC/PEA/KB(10) (Figure 5a).

In contrast, the intensities of PSCD⊃PEA/KB(10) in both directions increased through deformation, showing strain-induced phase separation (Figure S48). The orientation of PSCD⊃PEA/KB(10) was also observed from the higher intensity in the perpendicular direction at high ε. PSCD⊃PEA without KB also showed similar tendencies, indicating that the dethreading of the PEA secondary polymer contributed to the phase separation and orientation. Before deformation, PSCD⊃PEA/KB(10) had a peak at 30 nm corresponding to the diameter of the dispersed KB monoparticles. This peak decreased due to deformation and disappeared at ε = 80% strain, thereby showing the aggregation of KB. Consequently, the high sensitivity of PSCD⊃PEA/KB(10) was caused by strain-induced phase separation and KB aggregation (Figure 5b). Consequently, SAXS measurements revealed the relation between stress–strain sensing properties and the dynamics of polymer domains and KB aggregations.

CONCLUSION

We designed two kinds of nanocomposite materials with KB and movable cross-linked elastomers to achieve high toughness, high conductivity, and strain-sensing functions. One is SC/PEA/KB(w), which is obtained by mixing an SC elastomer, a linear polymer, and KB. The network structure

https://doi.org/10.1021/acspolymersau.3c00010
ACS Polym. Au 2023, 3, 394–405

consisting of linear polymers penetrating the SC network results in the high strength, stretchability, and conductivity of the material. The electrical resistance increases proportionally to the tensile strain, allowing for the application of this material as a stress−strain sensor. The responses of this material are stable for over 100 loading and unloading cycles. The other composite material is PSCD⊃PEA/KB(w), which is obtained by casting methods with high recyclability of the KP elastomer. The PS polymer and movable cross-links improve the mixability of KB to obtain a material with high strength, stretchability, and conductivity. PSCD⊃PEA/KB(w) can act as a highly sensitive stress−strain sensor due to its exponential increase in resistance with tensile strain. The high sensitivity of this material is derived from strain-induced phase separation and KB aggregation via dethreading of the polymer from CD rings. These network structures achieve highly stable and sensitive stress−strain sensors with excellent toughness, enabling very thin electrical devices to broaden their applications.

■ ASSOCIATED CONTENT

Supporting Information

The Supporting Information is available free of charge at https://pubs.acs.org/doi/10.1021/acspolymersau.3c00010.

Additional experimental details, materials, and methods, including photographs of experimental setup (PDF)

Movie for the demonstration of stress−strain sensor (MP4)

■ AUTHOR INFORMATION

Corresponding Authors

Yuta Nishina − *Research Core for Interdisciplinary Sciences and Graduate School of Natural Science and Technology, Okayama University, Kita-ku, Okayama 700-8530, Japan;* orcid.org/0000-0002-4958-1753; Email: nisina-y@cc.okayama-u.ac.jp

Yasutomo Uetsuji − *Department of Mechanical Engineering, Osaka Institute of Technology, Asahi-ku, Osaka 535-8585, Japan*; Email: yasutomo.uetsuji@oit.ac.jp

Go Matsuba − *Graduate School of Organic Materials Engineering, Yamagata University, Yonezawa, Yamagata 992-8510, Japan*; Email: gmatsuba@yz.yamagata-u.ac.jp

Yoshinori Takashima − *Department of Macromolecular Science, Graduate School of Science and Forefront Research Center for Fundamental Sciences, Osaka University, Toyonaka, Osaka 560-0043, Japan; Innovative Catalysis Science Division, Institute for Open and Transdisciplinary Research Initiatives (ICS-OTRI), Osaka University, Suita, Osaka 565-0871, Japan;* orcid.org/0000-0002-2620-3266; Email: takasima@chem.sci.osaka-u.ac.jp

Authors

Ryohei Ikura − *Department of Macromolecular Science, Graduate School of Science and Forefront Research Center for Fundamental Sciences, Osaka University, Toyonaka, Osaka 560-0043, Japan*

Kota Kajimoto − *Department of Macromolecular Science, Graduate School of Science, Osaka University, Toyonaka, Osaka 560-0043, Japan*

Junsu Park − *Department of Macromolecular Science, Graduate School of Science and Forefront Research Center for Fundamental Sciences, Osaka University, Toyonaka, Osaka 560-0043, Japan;* orcid.org/0000-0003-2557-904X

Shunsuke Murayama − *Graduate School of Organic Materials Engineering, Yamagata University, Yonezawa, Yamagata 992-8510, Japan*

Yusei Fujiwara − *Department of Mechanical Engineering, Osaka Institute of Technology, Asahi-ku, Osaka 535-8585, Japan*

Motofumi Osaki − *Department of Macromolecular Science, Graduate School of Science and Forefront Research Center for Fundamental Sciences, Osaka University, Toyonaka, Osaka 560-0043, Japan;* orcid.org/0000-0003-2874-9382

Tomohiro Suzuki − *Kanagawa Technical Center, Yushiro Chemical Industry Co., Ltd., Koza-gun, Kanagawa 253-0193, Japan*

Hidenori Shirakawa − *Kanagawa Technical Center, Yushiro Chemical Industry Co., Ltd., Koza-gun, Kanagawa 253-0193, Japan*

Yujiro Kitamura − *Kanagawa Technical Center, Yushiro Chemical Industry Co., Ltd., Koza-gun, Kanagawa 253-0193, Japan*

Hiroaki Takahashi − *Kanagawa Technical Center, Yushiro Chemical Industry Co., Ltd., Koza-gun, Kanagawa 253-0193, Japan*

Yasumasa Ohashi − *Kanagawa Technical Center, Yushiro Chemical Industry Co., Ltd., Koza-gun, Kanagawa 253-0193, Japan*

Seiji Obata − *Research Core for Interdisciplinary Sciences, Okayama University, Kita-ku, Okayama 700-8530, Japan*

Akira Harada − *SANKEN (The Institute of Scientific and Industrial Research), Osaka University, Ibaraki, Osaka 567-0047, Japan;* orcid.org/0000-0001-6177-1173

Yuka Ikemoto − *Japan Synchrotron Radiation Research Institute, Sayo-gun, Hyogo 679-5198, Japan*

Complete contact information is available at: https://pubs.acs.org/10.1021/acspolymersau.3c00010

Author Contributions

Ryohei Ikura: Writing − Original Draft (lead), Investigation (equal), Methodology (supporting); Kota Kajimoto: Investigation (equal), Writing − Original Draft (supporting); Junsu Park Methodology (supporting), Writing − Review & Editing (supporting); Shunsuke Murayama: Formal analysis (supporting); Yusei Fujiwara: Formal analysis (supporting); Motofumi Osaki: Methodology (supporting), Writing − Review & Editing (supporting); Tomohiro Suzuki: Resources (supporting); Hidenori Shirakawa: Resources (supporting); Yujiro Kitamura: Resources (supporting); Hiroaki Takahashi: Resources (supporting); Yasumasa Ohashi: Resources (lead); Seiji Obata: Formal analysis (supporting); Akira Harada: Writing − Review & Editing (supporting); Yuka Ikemoto: Formal analysis (equal), Writing − Review & Editing (supporting); Yuta Nishina: Formal analysis (equal), Writing − Review & Editing (supporting); Yasutomo Uetsuji: Formal analysis (equal), Writing − Review & Editing (supporting); Go Matsuba: Formal analysis (equal), Writing − Review & Editing (supporting); Yoshinori Takashima: Conceptualization (lead), Methodology (lead), Writing − Review & Editing (lead), Supervision (lead), Project administration (lead). CRediT: **Ryohei Ikura** investigation, methodology, writing-original draft; **Kota Kajimoto** investigation, methodology, writing-original draft; **Junsu Park** methodology, writing-review

https://doi.org/10.1021/acspolymersau.3c00010
ACS Polym. Au 2023, 3, 394−405

& editing; **Shunsuke Murayama** formal analysis; **Yusei Fujiwara** formal analysis; **Motofumi Osaki** methodology, writing-review & editing; **Tomohiro Suzuki** resources; **Hidenori Shirakawa** resources; **Yujiro Kitamura** resources; **Hiroaki Takahashi** resources; **Yasumasa Ohashi** resources; **Seiji Obata** formal analysis; **Akira Harada** writing-review & editing; **Yuka Ikemoto** formal analysis, writing-review & editing; **Yuta Nishina** formal analysis, writing-review & editing; **Yasutomo Uetsuji** formal analysis, writing-review & editing; **Go Matsuba** formal analysis, writing-review & editing; **Yoshinori Takashima** conceptualization, methodology, project administration, supervision, writing-review & editing.

Notes

The authors declare no competing financial interest.

■ ACKNOWLEDGMENTS

This research was funded by a Grant-in-Aid for Scientific Research on Innovative Area JP19H05714, JP19H05721, JP22H04548, and JP19H05717 from MEXT of Japan, the Kao Foundation for Arts and Sciences, and the Yazaki Memorial Foundation for Science. This work was also supported by JST, CREST Grant Number JPMJCR22L4, Japan. The authors appreciate Prof. Sadahito Aoshima and Prof. Arihiro Kanazawa (Graduate School of Science, Osaka University) for their support with the GPC measurements. The authors would like to thank the Analytical Instrument Faculty of the Graduate School of Science, Osaka University, for their support with the NMR, FT-IR, and TGA measurements. The authors also appreciate Mr. Ryuji Takata (Okayama University) for his support with electrical conductivity measurements. The authors would like to thank Dr. Keiichi Osaka and Dr. Noboru Ohta (SPring-8, JASRI) for the synchrotron radiation scattering measurements. The synchrotron radiation experiments were performed at BL19B2 (Proposal 2022B0578), BL40B2 (Proposal No. 2021A1593), and BL43IR (Proposal No. 2021A1608) of SPring-8 with the approval of the Japan Synchrotron Radiation Research Institute (JASRI).

■ REFERENCES

(1) Cochrane, C.; Koncar, V.; Lewandowski, M.; Dufour, C. Design and Development of a Flexible Strain Sensor for Textile Structures Based on a Conductive Polymer Composite. *sensors* **2007**, *7*, 473−492.

(2) Pang, C.; Lee, C.; Suh, K. Recent Advances in Flexible Sensors for Wearable and Implantable Devices. *J. APPL. POLYM. SCI.* **2013**, *130*, 1429−1441.

(3) Stoppa, M.; Chiolerio, A. Wearable Electronics and Smart Textiles: A Critical Review. *sensors* **2014**, *14*, 11957−11992.

(4) Kang, I.; Schulz, M. J.; Kim, J. H.; Shanov, V.; Shi, D. A Carbon Nanotube Strain Sensor for Structural Health Monitoring. *Smart Mater. Struct.* **2006**, *15*, 737−748.

(5) Liehr, S.; Lenke, P.; Wendt, M.; Krebber, K.; Seeger, M.; Thiele, E.; Metschies, H.; Gebreselassie, B.; Münich, J. C. Polymer Optical Fiber Sensors for Distributed Strain Measurement and Application in Structural Health Monitoring. *IEEE Sens. J.* **2009**, *9*, 1330−1338.

(6) Dong, K.; Peng, X.; Wang, Z. L. Fiber/Fabric-Based Piezoelectric and Triboelectric Nanogenerators for Flexible/Stretchable and Wearable Electronics and Artificial Intelligence. *Adv. Mater.* **2020**, *32*, No. 1902549.

(7) Kim, R.-H.; Kim, D.-H.; Xiao, J.; Kim, B. H.; Park, S.-I.; Panilaitis, B.; Ghaffari, R.; Yao, J.; Li, M.; Liu, Z.; Malyarchuk, V.; Kim, D. G.; Le, A.-P.; Nuzzo, R. G.; Kaplan, D. L.; Omenetto, F. G.; Huang, Y.; Kang, Z.; Rogers, J. A. Waterproof AlInGaP Optoelectronics on Stretchable Substrates with Applications in Biomedicine and Robotics. *Nat. Mater.* **2010**, *9*, 929−937.

(8) Markvicka, E. J.; Bartlett, M. D.; Huang, X.; Majidi, C. An Autonomously Electrically Self-Healing Liquid Metal−Elastomer Composite for Robust Soft-Matter Robotics and Electronics. *Nat. Mater.* **2018**, *17*, 618−624.

(9) Finkelmann, H.; Kim, S. T.; Muñoz, A.; Palffy-muhoray, P.; Taheri, B. Tunable Mirrorless Lasing in Cholesteric Liquid Crystalline Elastomers. *Adv. Mater.* **2001**, *13*, 1069−1072.

(10) Kotani, R.; Yokoyama, S.; Nobusue, S.; Yamaguchi, S.; Osuka, A.; Yabu, H.; Saito, S. Bridging Pico-to-Nanonewtons with a Ratiometric Force Probe for Monitoring Nanoscale Polymer Physics before Damage. *Nat. Commun.* **2022**, *13*, 303.

(11) Arsenault, A. C.; Clark, T. J.; von Freymann, G.; Cademartiri, L.; Sapienza, R.; Bertolotti, J.; Vekris, E.; Wong, S.; Kitaev, V.; Manners, I.; Wang, R. Z.; John, S.; Wiersma, D.; Ozin, G. A. From Colour Fingerprinting to the Control of Photoluminescence in Elastic Photonic Crystals. *Nat. Mater.* **2006**, *5*, 179−184.

(12) Sagara, Y.; Kato, T. Mechanically Induced Luminescence Changes in Molecular Assemblies. *Nat. Chem.* **2009**, *1*, 605−610.

(13) Davis, D. A.; Hamilton, A.; Yang, J.; Cremar, L. D.; Van Gough, D.; Potisek, S. L.; Ong, M. T.; Braun, P. V.; Martinez, T. J.; White, S. R.; Moore, J. S.; Sottos, N. R. Force-Induced Activation of Covalent Bonds in Mechanoresponsive Polymeric Materials. *Nature* **2009**, *459*, 68−72.

(14) Ducrot, E.; Chen, Y.; Bulters, M.; Sijbesma, R. P.; Creton, C. Toughening Elastomers with Sacrificial Bonds and Watching Them Break. *Science* **2014**, *344*, 186−189.

(15) Imato, K.; Kanehara, T.; Ohishi, T.; Nishihara, M.; Yajima, H.; Ito, M.; Takahara, A.; Otsuka, H. Mechanochromic Dynamic Covalent Elastomers : Quantitative Stress. *ACS Macro Lett.* **2015**, *4*, 1307−1311.

(16) Sagara, Y.; Karman, M.; Verde-Sesto, E.; Matsuo, K.; Kim, Y.; Tamaoki, N.; Weder, C. Rotaxanes as Mechanochromic Fluorescent Force Transducers in Polymers. *J. Am. Chem. Soc.* **2018**, *140*, 1584−1587.

(17) Fukawa, M.; Suzuki, K.; Furumi, S. Disappearance of Reflection Color by Photopolymerization of Lyotropic Cholesteric Liquid Crystals from Cellulose Derivatives. *J. Photopolym. Sci. Technol.* **2018**, *31*, 563−567.

(18) Miwa, E.; Watanabe, K.; Asai, F.; Seki, T.; Urayama, K.; Odent, J.; Raquez, J. M.; Takeoka, Y. Composite Elastomer Exhibiting a Stress-Dependent Color Change and High Toughness Prepared by Self-Assembly of Silica Particles in a Polymer Network. *ACS Appl. Polym. Mater.* **2020**, *2*, 4078−4089.

(19) Park, J.; You, I.; Shin, S.; Jeong, U. Material Approaches to Stretchable Strain Sensors. *ChemPhysChem* **2015**, *16*, 1155−1163.

(20) Alamusi; Hu, N.; Fukunaga, H.; Atobe, S.; Liu, Y.; Li, J. Piezoresistive Strain Sensors Made from Carbon Nanotubes Based Polymer Nanocomposites. *Sensors* **2011**, *11*, 10691−10723.

(21) Obitayo, W.; Liu, T. A Review : Carbon Nanotube-Based Piezoresistive Strain Sensors. *J. Sensors* **2012**, *2*, No. 652438.

(22) Ando, M.; Kawamura, H.; Kitada, H.; Sekimoto, Y.; Inoue, T.; Tajitsu, Y. Pressure-Sensitive Touch Panel Based on Piezoelectric Poly (L-Lactic Acid) Film. *Jpn. J. Appl. Phys.* **2013**, *52*, No. 09KD17.

(23) Gong, S.; Schwalb, W.; Wang, Y.; Chen, Y.; Tang, Y.; Si, J.; Shirinzadeh, B.; Cheng, W. A Wearable and Highly Sensitive Pressure Sensor with Ultrathin Gold Nanowires. *Nat. Commun.* **2014**, *5*, 3132.

(24) Petritz, A.; Karner-petritz, E.; Uemura, T.; Schäffner, P.; Araki, T.; Stadlober, B.; Sekitani, T. Imperceptible Energy Harvesting Device and Biomedical Sensor Based on Ultraflexible Ferroelectric Transducers and Organic Diodes. *Nat. Commun.* **2021**, *12*, 2399.

(25) Pu, X.; Liu, M.; Chen, X.; Sun, J.; Du, C.; Zhang, Y.; Zhai, J.; Hu, W.; Wang, Z. L. Ultrastretchable, Transparent Triboelectric Nanogenerator as Electronic Skin for Biomechanical Energy Harvesting and Tactile Sensing. *Sci. Adv.* **2017**, *3*, No. e1700015.

(26) Cohen, D. J.; Mitra, D.; Peterson, K.; Maharbiz, M. M. A Highly Elastic, Capacitive Strain Gauge Based on Percolating Nanotube Networks. *Nano Lett.* **2012**, *12*, 1821−1825.

https://doi.org/10.1021/acspolymersau.3c00010
ACS Polym. Au 2023, 3, 394−405

(27) Cai, L.; Song, L.; Luan, P.; Zhang, Q.; Zhang, N.; Gao, Q.; Zhao, D.; Zhang, X.; Tu, M.; Yang, F.; Zhou, W.; Fan, Q.; Luo, J.; Zhou, W.; Ajayan, P. M.; Xie, S. Super-Stretchable, Transparent Carbon Nanotube-Based Capacitive Strain Sensors for Human Motion Detection. *Sci. Rep.* **2013**, *3*, 3048.
(28) Fassler, A.; Majidi, C. Soft-Matter Capacitors and Inductors for Hyperelastic Strain Sensing and Stretchable Electronics. *Smart Mater. Struct.* **2013**, *22*, No. 055023.
(29) Frutiger, A.; Muth, J. T.; Vogt, D. M.; Menguc, Y.; Campo, A.; Valentine, A. D.; Walsh, C. J.; Lewis, J. A. Capacitive Soft Strain Sensors via Multicore − Shell Fiber Printing. *Adv. Mater.* **2015**, *27*, 2440−2446.
(30) Sekitani, T.; Zschieschang, U.; Klauk, H.; Someya, T. Flexible Organic Transistors and Circuits with Extreme Bending Stability. *Nat. Mater.* **2010**, *9*, 1015−1022.
(31) Lee, S.; Reuveny, A.; Reeder, J.; Lee, S.; Jin, H.; Liu, Q.; Yokota, T.; Sekitani, T.; Isoyama, T.; Abe, Y.; et al. A Transparent Bending-Insensitive Pressure Sensor. *Nat. Nanotechnol.* **2016**, *11*, 472−479.
(32) Chossat, J.; Park, Y.; Wood, R. J.; Duchaine, V. A Soft Strain Sensor Based on Ionic and Metal Liquids. *IEEE Sens. J.* **2013**, *13*, 3405−3414.
(33) Pan, L.; Chortos, A.; Yu, G.; Wang, Y.; Isaacson, S.; Allen, R.; Shi, Y.; Dauskardt, R.; Bao, Z. An Ultra-Sensitive Resistive Pressure Sensor Based on Hollow-Sphere Microstructure Induced Elasticity in Conducting Polymer Film. *Nat. Commun.* **2014**, *5*, 3002.
(34) Choi, D. Y.; Kim, M. H.; Oh, Y. S.; Jung, S.; Jung, J. H.; Sung, H. J.; Lee, H. W.; Lee, H. M. Highly Stretchable, Hysteresis-Free Ionic Liquid-Based Strain Sensor for Precise Human Motion Monitoring. *ACS Appl. Mater. Interfaces* **2017**, *9*, 1770−1780.
(35) Yang, Z.; Pang, Y.; Han, X.; Yang, Y.; Ling, J.; Jian, M.; Zhang, Y.; Yang, Y.; Ren, T. Graphene Textile Strain Sensor with Negative Resistance Variation for Human Motion Detection. *ACS Nano* **2018**, *12*, 9134−9141.
(36) Yang, J. C.; Kim, J.; Oh, J.; Kwon, S. Y.; Sim, J. Y.; Kim, D. W.; Choi, H. B.; Park, S. Microstructured Porous Pyramid-Based Ultrahigh Sensitive Pressure Sensor Insensitive to Strain and Temperature. *ACS Appl. Mater. Interfaces* **2019**, *11*, 19472−19480.
(37) Kim, Y.; Kim, Y.; Lee, C.; Kwon, S. Thin Polysilicon Gauge for Strain Measurement of Structural Elements. *IEEE Sens. J.* **2010**, *10*, 1320−1327.
(38) Won, S. M.; Kim, H. S.; Lu, N.; Kim, D. G.; Del Solar, C.; Duenas, T.; Ameen, A.; Rogers, J. A. Erratum: Piezoresistive Strain Sensors and Multiplexed Arrays Using Assemblies of Single-Crystalline Silicon Nanoribbons on Plastic Substrates. *IEEE Trans. Electron Devices* **2012**, *59*, 520.
(39) Knite, M.; Teteris, V.; Kiploka, A.; Kaupuzs, J. Polyisoprene-Carbon Black Nanocomposites as Tensile Strain and Pressure Sensor Materials. *Sens. Actuators* **2004**, *110*, 142−149.
(40) Thostenson, E. T.; Chou, T. Carbon Nanotube Networks : Sensing of Distributed Strain and Damage for Life Prediction and Self Healing. *Adv. Mater.* **2006**, *18*, 2837−2841.
(41) Yoshimura, K.; Nakano, K.; Okamoto, K.; Miyake, T. Sensors and Actuators A : Physical Mechanical and Electrical Properties in Porous Structure of Ketjenblack/Silicone − Rubber Composites. *Sensors Actuators A. Phys.* **2012**, *180*, 55−62.
(42) Lu, N.; Lu, C.; Yang, S.; Rogers, J. Highly Sensitive Skin-Mountable Strain Gauges Based Entirely on Elastomers. *Adv. Funct. Mater.* **2012**, *22*, 4044−4050.
(43) Muth, J. T.; Vogt, D. M.; Truby, R. L.; Menguc, Y.; Kolesky, D. B.; Wood, R. J.; Lewis, J. A. Embedded 3D Printing of Strain Sensors within Highly Stretchable Elastomers. *Adv. Mater.* **2014**, *26*, 6307−6312.
(44) Rahimi, R.; Ochoa, M.; Yu, W.; Ziaie, B. Highly Stretchable and Sensitive Unidirectional Strain Sensor via Laser Carbonization. *ACS Appl. Mater. Interfaces* **2015**, *7*, 4463−4470.
(45) Hu, N.; Karube, Y.; Yan, C.; Masuda, Z.; Fukunaga, H. Tunneling Effect in a Polymer/Carbon Nanotube Nanocomposite Strain Sensor. *Acta Mater.* **2008**, *56*, 2929−2936.
(46) Bauhofer, W.; Kovacs, J. Z. A Review and Analysis of Electrical Percolation in Carbon Nanotube Polymer Composites. *Compos. Sci. Technol.* **2009**, *69*, 1486−1498.
(47) Ma, P.; Siddiqui, N. A.; Marom, G.; Kim, J. Composites : Part A Dispersion and Functionalization of Carbon Nanotubes for Polymer-Based Nanocomposites : A Review. *Compos. Part A* **2010**, *41*, 1345−1367.
(48) Byrne, B. M. T.; Gun'ko, Y. K. Recent Advances in Research on Carbon Nanotube − Polymer Composites. *Adv. Mater.* **2010**, *22*, 1672−1688.
(49) Lipomi, D. J.; Vosgueritchian, M.; Tee, B. C.; Hellstrom, S. L.; Lee, J. A.; Fox, C. H.; Bao, Z. Skin-like Pressure and Strain Sensors Based on Transparent Elastic Films of Carbon Nanotubes. *Nat. Nanotechnol.* **2011**, *6*, 788−792.
(50) Yamada, T.; Hayamizu, Y.; Yamamoto, Y.; Yomogida, Y.; Izadi-najafabadi, A.; Futaba, D. N.; Hata, K. A Stretchable Carbon Nanotube Strain Sensor for Human-Motion Detection. *Nat. Nanotechnol.* **2011**, *6*, 296−301.
(51) Hu, N.; Itoi, T.; Akagi, T.; Kojima, T.; Xue, J.; Yan, C.; Atobe, S.; Fukunaga, H.; Yuan, W.; Ning, H.; Surina; Liu, Y.; Alamusi. Ultrasensitive Strain Sensors Made from Metal-Coated Carbon Nanofiller/Epoxy Composites. *Carbon N. Y.* **2013**, *51*, 202−212.
(52) Deng, H.; Lin, L.; Ji, M.; Zhang, S.; Yang, M.; Fu, Q. Progress on the Morphological Control of Conductive Network in Conductive Polymer Composites and the Use as Electroactive Multifunctional Materials. *Prog. Polym. Sci.* **2014**, *39*, 627−655.
(53) Amjadi, M.; Yoon, Y. J.; Park, I. Ultra-Stretchable and Skin-Mountable Strain Sensors Using Carbon Nanotubes − Ecoflex Nanocomposites. *Nanotechnology* **2015**, *26*, No. 375501.
(54) Liao, M.; Wan, P.; Wen, J.; Gong, M.; Wu, X.; Wang, Y.; Shi, R.; Zhang, L. Wearable, Healable, and Adhesive Epidermal Sensors Assembled from Mussel-Inspired Conductive Hybrid Hydrogel Framework. *Adv. Funct. Mater.* **2017**, *27*, No. 1703852.
(55) Kuilla, T.; Bhadra, S.; Yao, D.; Kim, N. H.; Bose, S.; Lee, J. H. Progress in Polymer Science Recent Advances in Graphene Based Polymer Composites. *Prog. Polym. Sci.* **2010**, *35*, 1350−1375.
(56) Sengupta, R.; Bhattacharya, M.; Bandyopadhyay, S.; Bhowmick, A. K. Progress in Polymer Science A Review on the Mechanical and Electrical Properties of Graphite and Modified Graphite Reinforced Polymer Composites. *Prog. Polym. Sci.* **2011**, *36*, 638−670.
(57) Boland, C. S.; Khan, U.; Backes, C.; O'Neill, A.; McCauley, J.; Duane, S.; Shanker, R.; Liu, Y.; Jurewicz, I.; Dalton, A. B.; Coleman, J. N. Terms of Use Bodily Motion Sensors Based on Graphene A Rubber Composites. *ACS Nano* **2014**, *8*, 8819−8830.
(58) Wang, Y.; Wang, L.; Yang, T.; Li, X.; Zang, X.; Zhu, M.; Wang, K.; Wu, D.; Zhu, H. Wearable and Highly Sensitive Graphene Strain Sensors for Human Motion Monitoring. *Adv. Funct. Mater.* **2014**, *24*, 4666−4670.
(59) Qin, Y.; Peng, Q.; Ding, Y.; Lin, Z.; Wang, C.; Li, Y.; Xu, F.; Li, J.; Yuan, Y.; He, X.; Li, Y. Mechanically Flexible Graphene/Polyimide Nanocomposite Foam for Strain Sensor Application. *ACS Nano* **2015**, *9*, 8933−8941.
(60) Boland, C. S.; Khan, U.; Ryan, G.; Barwich, S.; Charifou, R.; Harvey, A.; Backes, C.; Li, Z.; Ferreira, M. S.; Möbius, M. E.; Young, R. J.; Coleman, J. N. Sensitive Electromechanical Sensors Using Viscoelastic Graphene-Polymer Nanocomposites. *Science* **2016**, *354*, 1257−1260.
(61) Liu, H.; Gao, J.; Huang, W.; Dai, K.; Zheng, G.; Liu, C.; Shen, C.; Yan, X.; Guo, J.; Guo, Z. Electrically Conductive Strain Sensing Polyurethane Nanocomposites with Synergistic Carbon Nanotubes and Graphene Bifillers. *Nanoscale* **2016**, *8*, 12977−12989.
(62) Yan, C.; Wang, J.; Kang, W.; Cui, M.; Wang, X.; Foo, C. Y.; Chee, K. J.; Lee, P. S. Highly Stretchable Piezoresistive Graphene − Nanocellulose Nanopaper for Strain Sensors. *Adv. Mater.* **2014**, *26*, 2022−2027.
(63) Chun, K.; Oh, Y.; Rho, J.; Ahn, J.; Kim, Y.; Choi, H. R.; Baik, S. Highly Conductive, Printable and Stretchable Composite Films of Carbon Nanotubes and Silver. *Nat. Nanotechnol.* **2010**, *5*, 853−857.

https://doi.org/10.1021/acspolymersau.3c00010
ACS Polym. Au 2023, 3, 394−405

(64) Xu, F.; Zhu, Y. Highly Conductive and Stretchable Silver Nanowire Conductors. *Adv. Mater.* **2012**, *24*, 5117−5122.
(65) Park, M.; Im, J.; Shin, M.; Min, Y.; Park, J.; Cho, H.; Park, S.; Shim, M.; Jeon, S.; Chung, D.; Bae, J.; Park, J.; Jeong, U.; Kim, K. Highly Stretchable Electric Circuits from a Composite Material of Silver Nanoparticles and Elastomeric Fibres. *Nat. Nanotechnol.* **2012**, *7*, 803−809.
(66) Kim, Y.; Zhu, J.; Yeom, B.; Di Prima, M.; Su, X.; Kim, J.-G.; Yoo, S. J.; Uher, C.; Kotov, N. A. Stretchable Nanoparticle Conductors with Self-Organized Conductive Pathways. *Nature* **2013**, *500*, 59−63.
(67) Amjadi, M.; Pichitpajongkit, A.; Lee, S.; Ryu, S.; Park, I. Highly Stretchable and Sensitive Strain Sensor Based on Silver Nanowire−Elastomer Nanocomposite. *ACS Nano* **2014**, *8* (5), 5154−5163.
(68) Jeong, Y. R.; Park, H.; Jin, S. W.; Hong, S. Y.; Lee, S.; Ha, J. S. Highly Stretchable and Sensitive Strain Sensors Using Fragmentized Graphene Foam. *Adv. Funct. Mater.* **2015**, *25*, 4228−4236.
(69) Pang, Y.; Tian, H.; Tao, L.; Li, Y.; Wang, X.; Deng, N.; Yang, Y.; Ren, T. Flexible, Highly Sensitive, and Wearable Pressure and Strain Sensors with Graphene Porous Network Structure. *ACS Appl. Mater. Interfaces* **2016**, *8*, 26458−26462.
(70) Liu, T.; Li, C.; Yao, H.; Sun, F.; Wang, L.; Yao, B.; Xu, J.; Fu, J. Extremely strengthening fatigue resistance, elastic restorability and thermodynamic stability of a soft transparent self-healing network based on a dynamic molecular confinement-induced bioinspired nanostructure. *Mater. Hori.* **2023**, *10*, 2968−2979.
(71) Sun, F.; Liu, L.; Liu, T.; Wang, X.; Qi, Q.; Hang, Z.; Chen, K.; Xu, J.; Fu, J. Vascular smooth muscle-inspired architecture enables soft yet tough self-healing materials for durable capacitive strain-sensor. *Nat. Commun.* **2023**, *14*, 130.
(72) Matsuhisa, N.; Inoue, D.; Zalar, P.; Jin, H.; Matsuba, Y.; Itoh, A.; Yokota, T.; Hashizume, D.; Someya, T. Printable Elastic Conductors by in Situ Formation of Silver Nanoparticles from Silver Flakes. *Nat. Mater.* **2017**, *16*, 834−840.
(73) Wang, T.; Zhang, Y.; Liu, Q.; Cheng, W.; Wang, X.; Pan, L.; Xu, B.; Xu, H. A Self-Healable, Highly Stretchable, and Solution Processable Conductive Polymer Composite for Ultrasensitive Strain and Pressure Sensing. *Adv. Funct. Mater.* **2018**, *28*, No. 1705551.
(74) Wang, Z.; Chen, J.; Cong, Y.; Zhang, H.; Xu, T.; Nie, L.; Fu, J. Ultrastretchable Strain Sensors and Arrays with High Sensitivity and Linearity Based on Super Tough Conductive Hydrogels. *Chem. Mater.* **2018**, *30*, 8062−8069.
(75) Jiang, Y.; Zhang, Z.; Wang, Y.-X.; Li, D.; Coen, C.-T.; Hwaun, E.; Chen, G.; Wu, H.-C.; Zhong, D.; Niu, S.; Wang, W.; Saberi, A.; Lai, J.-C.; Wu, Y.; Wang, Y.; Trotsyuk, A. A.; Loh, K. Y.; Shih, C.-C.; Xu, W.; Liang, K.; Zhang, K.; Bai, Y.; Gurusankar, G.; Hu, W.; Jia, W.; Cheng, Z.; Dauskardt, R. H.; Gurtner, G. C.; Tok, J. B.-H.; Deisseroth, K.; Soltesz, I.; Bao, Z. Topological Supramolecular Network Enabled High-Conductivity, Stretchable Organic Bioelectronics. *Science* **2022**, *375*, 1411−1417.
(76) Zhang, Y.; Lee, K. H.; Anjum, D. H.; Sougrat, R.; Jiang, Q.; Kim, H.; Alshareef, H. N. MXenes Stretch Hydrogel Sensor Performance to New Limits. *Sci. Adv.* **2018**, *4*, No. eaat0098.
(77) Liu, S.; Li, L. Ultrastretchable and Self-Healing Double-Network Hydrogel for 3D Printing and Strain Sensor. *ACS Appl. Mater. Interfaces* **2017**, *9*, 26429−26437.
(78) Cao, Z.; Liu, H.; Jiang, L. Transparent, Mechanically Robust, and Ultrastable Ionogels Enabled by Hydrogen Bonding between Elastomers and Ionic Liquids. *Mater. Horizons* **2020**, *7*, 912−918.
(79) Li, T.; Wang, Y.; Li, S.; Liu, X.; Sun, J. Mechanically Robust, Elastic, and Healable Ionogels for Highly Sensitive Ultra-Durable Ionic Skins. *Adv. Mater.* **2020**, *32*, No. 2002706.
(80) Gong, J. P.; Katsuyama, Y.; Kurokawa, T.; Osada, Y. Double-Network Hydrogels with Extremely High Mechanical Strength. *Adv. Mater.* **2003**, *15*, 1155−1158.
(81) Myung, D.; Waters, D.; Wiseman, M.; Duhamel, P.-E.; Noolandi, J.; Ta, C. N.; Frank, C. W. Progress in the Development of Interpenetrating Polymer Network Hydrogels. *Polym. Adv. Technol.* **2008**, *19*, 647−657.
(82) Sun, J.-Y.; Zhao, X.; Illeperuma, W. R. K.; Chaudhuri, O.; Oh, K. H.; Mooney, D. J.; Vlassak, J. J.; Suo, Z. Highly Stretchable and Tough Hydrogels. *Nature* **2012**, *489*, 133−136.
(83) Sato, K.; Nakajima, T.; Hisamatsu, T.; Nonoyama, T.; Kurokawa, T.; Gong, J. P. Phase-Separation-Induced Anomalous Stiffening, Toughening, and Self-Healing of Polyacrylamide Gels. *Adv. Mater.* **2015**, *27*, 6990−6998.
(84) Haraguchi, K.; Takehisa, T. Nanocomposite Hydrogels: AUnique Organic-Inorganic Network Structure with Extraordinary Mechanical, Optical, and Swelling/De-Swelling Properties. *Adv. Mater.* **2002**, *14*, 1120−1124.
(85) Burnworth, M.; Tang, L.; Kumpfer, J. R.; Duncan, A. J.; Beyer, F. L.; Fiore, G. L.; Rowan, S. J.; Weder, C. Optically Healable Supramolecular Polymers. *Nature* **2011**, *472*, 334−337.
(86) Wang, S.; Urban, M. W. Self-Healing Polymers. *Nat. Rev. Mater.* **2020**, *5*, 562−583.
(87) Park, J.; Murayama, S.; Osaki, M.; Yamaguchi, H.; Harada, A.; Matsuba, G.; Takashima, Y. Extremely Rapid Self-Healable and Recyclable Supramolecular Materials through Planetary Ball Milling and Host−Guest Interactions. *Adv. Mater.* **2020**, *32*, No. 2002008.
(88) Zhao, X.; Chen, X.; Yuk, H.; Lin, S.; Liu, X.; Parada, G. Soft Materials by Design: Unconventional Polymer Networks Give Extreme Properties. *Chem. Rev.* **2021**, *121*, 4309−4372.
(89) Chen, Y.; Kushner, A. M.; Williams, G. A.; Guan, Z. Multiphase Design of Autonomic Self-Healing Thermoplastic Elastomers. *Nat. Chem.* **2012**, *4*, 467−472.
(90) Sun, T. L.; Kurokawa, T.; Kuroda, S.; Ihsan, A. B.; Akasaki, T.; Sato, K.; Haque, M. A.; Nakajima, T.; Gong, J. P. Physical Hydrogels Composed of Polyampholytes Demonstrate High Toughness and Viscoelasticity. *Nat. Mater.* **2013**, *12*, 932−937.
(91) Kakuta, T.; Takashima, Y.; Nakahata, M.; Otsubo, M.; Yamaguchi, H.; Harada, A. Preorganized Hydrogel: Self-Healing Properties of Supramolecular Hydrogels Formed by Polymerization of Host-Guest-Monomers That Contain Cyclodextrins and Hydrophobic Guest Groups. *Adv. Mater.* **2013**, *25*, 2849−2853.
(92) Roy, N.; Bruchmann, B.; Lehn, J. M. DYNAMERS: Dynamic Polymers as Self-Healing Materials. *Chem. Soc. Rev.* **2015**, *44*, 3786−3807.
(93) Urban, M. W.; Davydovich, D.; Yang, Y.; Demir, T.; Zhang, Y.; Casabianca, L. Key-and-Lock Commodity Self-Healing Copolymers. *Science* **2018**, *362*, 220−225.
(94) Yanagisawa, Y.; Nan, Y.; Okuro, K.; Aida, T. Mechanically Robust, Readily Repairable Polymers via Tailored Noncovalent Cross-Linking. *Science* **2018**, *359*, 72−76.
(95) Miwa, Y.; Taira, K.; Kurachi, J.; Udagawa, T.; Kutsumizu, S. A Gas-Plastic Elastomer That Quickly Self-Heals Damage with the Aid of CO 2 Gas. *Nat. Commun.* **2019**, *10*, 1828.
(96) Wang, H.; Yang, Y.; Nishiura, M.; Higaki, Y.; Takahara, A.; Hou, Z. Synthesis of Self-Healing Polymers by Scandium-Catalyzed Copolymerization of Ethylene and Anisylpropylenes. *J. Am. Chem. Soc.* **2019**, *141*, 3249−3257.
(97) Okumura, Y.; Ito, K. The Polyrotaxane Gel: A Topological Gel by Figure-of-Eight Cross-Links. *Adv. Mater.* **2001**, *13*, 485−487.
(98) Arai, T.; Jang, K.; Koyama, Y.; Asai, S.; Takata, T. Versatile Supramolecular Cross-Linker: A Rotaxane Cross-Linker That Directly Endows Vinyl Polymers with Movable Cross-Links. *Chem. - A Eur. J.* **2013**, *19*, 5917−5923.
(99) Kawai, Y.; Park, J.; Ishii, Y.; Urakawa, O.; Murayama, S.; Ikura, R.; Osaki, M.; Ikemoto, Y.; Yamaguchi, H.; Harada, A.; Inoue, T.; Washizu, H.; Matsuba, G.; Takashima, Y. Preparation of Dual-Cross Network Polymers by the Knitting Method and Evaluation of Their Mechanical Properties. *NPG Asia Mater.* **2022**, *14*, 32.
(100) Ikura, R.; Murayama, S.; Park, J.; Ikemoto, Y.; Osaki, M.; Yamaguchi, H.; Harada, A.; Matsuba, G.; Takashima, Y. Fabrication and Mechanical Properties of Knitted Dissimilar Polymeric Materials with Movable Cross-Links. *Mol. Syst. Des. Eng.* **2022**, *7*, 733−745.
(101) Tsuchiya, H.; Asaki, Y.; Sinawang, G.; Asoh, T.; Osaki, M.; Park, J.; Ikemoto, Y.; Yamaguchi, H.; Harada, A.; Uyama, H.; Takashima, Y. Cellulose Nanofiber Composite Polymeric Materials

with Reversible and Movable Cross-Links and Evaluation of Their Mechanical Properties. *ACS Appl. Polym. Mater.* **2022**, *4*, 403−412.
(102) Jin, C.; Park, J.; Shirakawa, H.; Osaki, M.; Ikemoto, Y.; Yamaguchi, H.; Takahashi, H.; Ohashi, Y.; Harada, A.; Matsuba, G.; Takashima, Y. Synergetic Improvement in the Mechanical Properties of Polyurethanes with Movable Crosslinking and Hydrogen Bonds. *Soft Matter* **2022**, *18*, 5027−5036.
(103) Bin Imran, A.; Esaki, K.; Gotoh, H.; Seki, T.; Ito, K.; Sakai, Y.; Takeoka, Y. Extremely Stretchable Thermosensitive Hydrogels by Introducing Slide-Ring Polyrotaxane Cross-Linkers and Ionic Groups into the Polymer Network. *Nat. Commun.* **2014**, *5*, 5124.
(104) Noda, Y.; Hayashi, Y.; Ito, K. From Topological Gels to Slide-Ring Materials. *J. Appl. Polym. Sci.* **2014**, *131*, 40509.
(105) Sawada, J.; Aoki, D.; Uchida, S.; Otsuka, H.; Takata, T. Synthesis of Vinylic Macromolecular Rotaxane Cross-Linkers Endowing Network Polymers with Toughness. *ACS Macro Lett.* **2015**, *4*, 598−601.
(106) Kureha, T.; Aoki, D.; Hiroshige, S.; Iijima, K.; Aoki, D.; Takata, T.; Suzuki, D. Decoupled Thermo- and PH-Responsive Hydrogel Microspheres Cross-Linked by Rotaxane Networks. *Angew. Chem., Int. Ed.* **2017**, *56*, 15393−15396.
(107) Gotoh, H.; Liu, C.; Imran, A. B.; Hara, M.; Seki, T.; Mayumi, K.; Ito, K.; Takeoka, Y. Optically Transparent, High-Toughness Elastomer Using a Polyrotaxane Cross-Linker as a Molecular Pulley. *Sci. Adv.* **2018**, *4*, No. eaat7629.
(108) Ikura, R.; Park, J.; Osaki, M.; Yamaguchi, H.; Harada, A.; Takashima, Y. Supramolecular Elastomers with Movable Cross-Linkers Showing High Fracture Energy Based on Stress Dispersion. *Macromolecules* **2019**, *52*, 6953−6962.
(109) Ikura, R.; Ikemoto, Y.; Osaki, M.; Yamaguchi, H.; Harada, A.; Takashima, Y. Preparation of Hydrophilic Polymeric Materials with Movable Cross-Linkers and Their Mechanical Property. *Polymer* **2020**, *196*, No. 122465.
(110) Zhao, D.; Zhang, Z.; Zhao, J.; Liu, K.; Liu, Y.; Li, G.; Zhang, X.; Bai, R.; Yang, X.; Yan, X. A Mortise-and-Tenon Joint Inspired Mechanically Interlocked Network. *Angew. Chem., Int. Ed.* **2021**, *60*, 16224−16229.
(111) Somani, R. H.; Shaw, M. T. Miscibility of Acrylic Polymers in Polystyrene by Melt Titration. *Macromolecules* **1981**, *14*, 1549−1554.
(112) Evaluation between mechanical properties of SC/PEA/KB(*w*) and morphology of KB through multiscale finite element (FEM) simulation (Figure S40−S42; Tables S10−S11).

https://doi.org/10.1021/acspolymersau.3c00010
ACS Polym. Au 2023, 3, 394−405